CORROSION SCIENCE AND TECHNOLOGY, Vol.5, No.6(2006), pp.206~212

The Tarnish Process of Silver in H_2S Environments

†H. Kim and J.H. Payer[1]

School of Materials Science and Engineering Hongik University
300 Sinan-ri, Chochiwon-eup, Youngi-gun, Chungnam, Korea, 339-701
[1]Department Materials Science and Engineering Case Western Reserve University
10900 Euclid Avenue, Cleveland, Ohio 44106

The effects of sub-ppm levels of H_2S and the adsorbed water on the atmospheric corrosion of silver were studied with *In situ* weight balance to study the effect of the adsorbed water on the kinetic behavior and to determine the rate-controlling step, with XPS to analyze the tarnish film, and with calculation of phase equilibrium to predict the stable solid phase, the concentrations of dissolved species (Ag^+, H^+, S^{2-}, HS^-) and the equilibrium potentials ($E_{Ag^+/Ag}$, E_{H^+/H_2}, $E_{O_2/O^{2-}}$). The results of weight measurements showed that oxygen was required for the sulfidation of silver in 100 ppb H_2S and humidified environments enhanced the tarnished rate and oxidizing power. In addition, the rate determining step for tarnishing silver was shown to be changed to transport though the tarnish film

Keywords *: silver, quartz crystal mass balance, relative humidity*

1. Introduction

Silver has been used for electronic connector materials, solder, batteries and decorating materials because of its electrical and thermal properties. Hence, the atmospheric corrosion of silver has been studied with an emphasis on the effect of humidity effect, the effect of gas and the kinetic mechanism.

Fiaud and Guinement[1)] conducted indoor laboratory studies on the corrosion of silver in atmospheric environments of controlled relative humidity and pollutant gases, reporting that the corrosion product was silver sulfide and that the kinetic behavior conformed to a parabolic law. This does not agree with D. Simon's result[2)] that the kinetic behavior conformed to linear law. Kuhn and Kelsall[3)] calculated the stable phase in Ag - H_2S - O_2 and Ag - H_2S - O_2 - H_2O with their thermodynamic data, indicating that silver sulfate was stable instead of silver sulfide. This difference between Kuhn & Kelsall's result and Fiaud & Guinement's experimental result was explained by a large barrier for the formation of sulfate from sulfide.

In addition, the reaction process is controvertible. Abbott[4)] proposed that the sulfidation mechanism of silver exposed to hydrogen sulfide with ambient air was as follows:

$$8H_2S + 4O_2 \rightarrow S_8 + H_2O \quad (1)$$

$$S_8 + 16Ag \rightarrow 8Ag_2S \quad (2)$$

According to Graedel,[5)] the sulfidation mechanisms were proposed depending on the humidity. At low relative humidity, H_2S gas reacted with silver metal directly, but at high relative humidity, dissolved species (HS^-, S^{2-}) from H_2S gas reacted with silver (*i.e.*, $16Ag + H_2S$ R $Ag_2S + H_2(g)$). Volpe and Peterson[6] exposed silver to dry air containing H_2S (100 ppb - 400 ppb) in flowing gas and proposed the following reaction:

$$Ag + H_2S + 1/2O_2 \rightarrow Ag_2S + H_2O \quad (3)$$

However, according to Phipps and Rice,[7)] at low relative humidity (R.H. < 40%, the ad-layer thickness < 1 monolayer), it is difficult to hydrate ions, but at high relative humidity (R.H. < 65%, the ad-layer thickness < 3 monolayer), the behavior of the adsorbed water layer approaches that of a bulk water layer and electrochemical processes are possible.

In this study, to get a better understanding of the sulfidation process of silver in H_2S environments, the effect of relative humidity, oxygen or H_2S was studied with an *in situ* weight balance and XPS. In addition, electrolyte thermodynamics were applied by assuming that the bulk

†Corresponding author: heesankim@yahoo.co.kr

thermodynamical properties are the same as the surface in order to explain the tarnishing process.

2. Experimentals

Silver was deposited on the front surface of a crystal by evaporation at Midwest Research Technologies, Inc. to a thickness of 5000 Å. Prior to the deposition, the back surface was masked and gold, previously deposited on the front side was stripped by aquaregia solution, cleaned with distilled water and acetone alternatively three times and dried with N_2 gas. The silver coated crystal was kept in desiccant before and after exposure. Before the exposure, the surface of silver was analyzed with XPS. The adsorbed species, such as adventitious hydrocarbon, $(OH)_{ad}$, adsorbed oxygen were detected, but the oxide was not detected.

The sub-ppm level of concentration was controlled using a permeation tube. In order to get reproducible results, the concentrations of H_2S, the relative humidity and the temperature in chamber were monitored during the exposure. The temperature of the chamber was kept at 25 ± 0.1 ℃ and the flow rate was 1 *l*/min. The purified air supplied by an air supply or nitrogen (with 99.99% purity) from nitrogen cylinder was used as a carrier gas. The concentration of H_2S was maintained at 100±5 ppb during the exposure, while the concentrations of undesired gases in the purified air were less than 1 ppb for SO_2, 0.1 ppb for H_2S, 1 ppb for NO, 1 ppb for NO_2, 1 ppb for O_2, 1.8×10^3 ppb for CO_2 and 100 ppb for CO.[8] The details of the mixed flowing gas system were described in other papers.[9]

An *in situ* mass measurement technique with high mass sensitivity (≅10 ng/cm^2), quartz crystal microbalance (QCM), with high mass sensitivity(≅10 ng/cm^2) was employed to monitor the mass change during exposure to part per billion pollutants and during the transition between wet and dry environments. The block diagram of the circuitry elements and the description of the particular circuitry employed are given elsewhere.[10] The circuitry designed for the oscillation of a 5 MHz quartz crystal was modified for the oscillation of a 6 MHz quartz crystal. In addition, the newly designed QCM was calibrated by the potentiostatic method with the following experimental conditions[11]: 0.2 M $HClO_4 + 10^{-3}$ M $AgNO_3$ at 0.0 V (SHE). The result (12.21 ng/Hz-cm^2) agreed well with the theoretically calculated value (12.26 ng/Hz-cm^2). The holder was made of polychloro-trifluoro ethylene to minimize the mass change due to the chemical reaction between the holder, silver and gases. Viton O-ring was placed on both sides of the crystal to ensure proper sealing and to minimize the residual stress since the frequency of the crystal can be affected by pressure as well as mass change.

The tarnish film after the exposure was analyzed on a PHI 5400 XPS system (Perkin Elmer Corp.) equipped with a water cooled Mg-anode (Mg-Kα: 1253.6eV and FWHM (full width at half maximum): 0.7eV) at total power dissipation of 400 watts (15KV, 26.7mA). The sample stage was positioned such that the photoelectron emitted at an angle of 45 degrees to the plane of silver surface entered the analyzer through a 1 mm×4 mm aperture. The spectrometer was calibrated with two reference points (Ag-$3d_{5/2}$: 368.3eV and C-1s: 284.5eV) to minimize the error due to the drift of the spectrometer with assumption that the shift of energy due to charging effects was negligible. In order to analyze the inside of the tarnish film, the differentially pumped argon ion gun (4KV, 2mA ions) of the XPS system was utilized. The calibration of the removal rate was accomplished by sputtering through the thickness of a Ta_2O_5 standard (1.8nm/min.).

The surface morphology after exposure was observed by Field Emission Scanning Electron Microscopy (Model S-4500, Hitachi Ltd.) with an accelerating voltage of 5 KV to provide information on the tarnishing process. The sample stage was positioned such that the incident electron collided with silver surface at an angle of 40 degrees to the plane of the silver surface to maximize the spatial resolution. The morphology could be observed with maximum magnification of 100 KX because of utilization of field emission as an electron source.

3. Results

3.1 Analysis of tarnish film with XPS

Fig. 1 shows the XPS spectrum of the tarnish film formed on silver exposed to 100 ppb H_2S with air containing 75% R.H. for 72 hours. The peaks of sulfur-2p were detected at 161.8 and 161.0 eV from the film surface indicating sulfide. No peak indicating sulfite or sulfate was detected before or after sputtering. The Auger parameter (724.8eV) calculated from the silver-$3d_{5/2}$ peak (B.E. = 368.2eV) and Ag-M_4VV (K.E. = 357.7eV) detected correspond to that of silver sulfide. The Auger parameter was shifted to that for silver metal as the intensity of sulfur-2p peaks decreased with sputtering. The broad peak of oxygen-1s on the surface disappeared after sputtering. This peak is thought to result from $(OH)_{ad}$, water and adsorbed oxygen. No oxygen-1s peak indicating the presence of oxide was detected before or after sputtering. Adventitious carbon also appeared on the surface and disappeared after

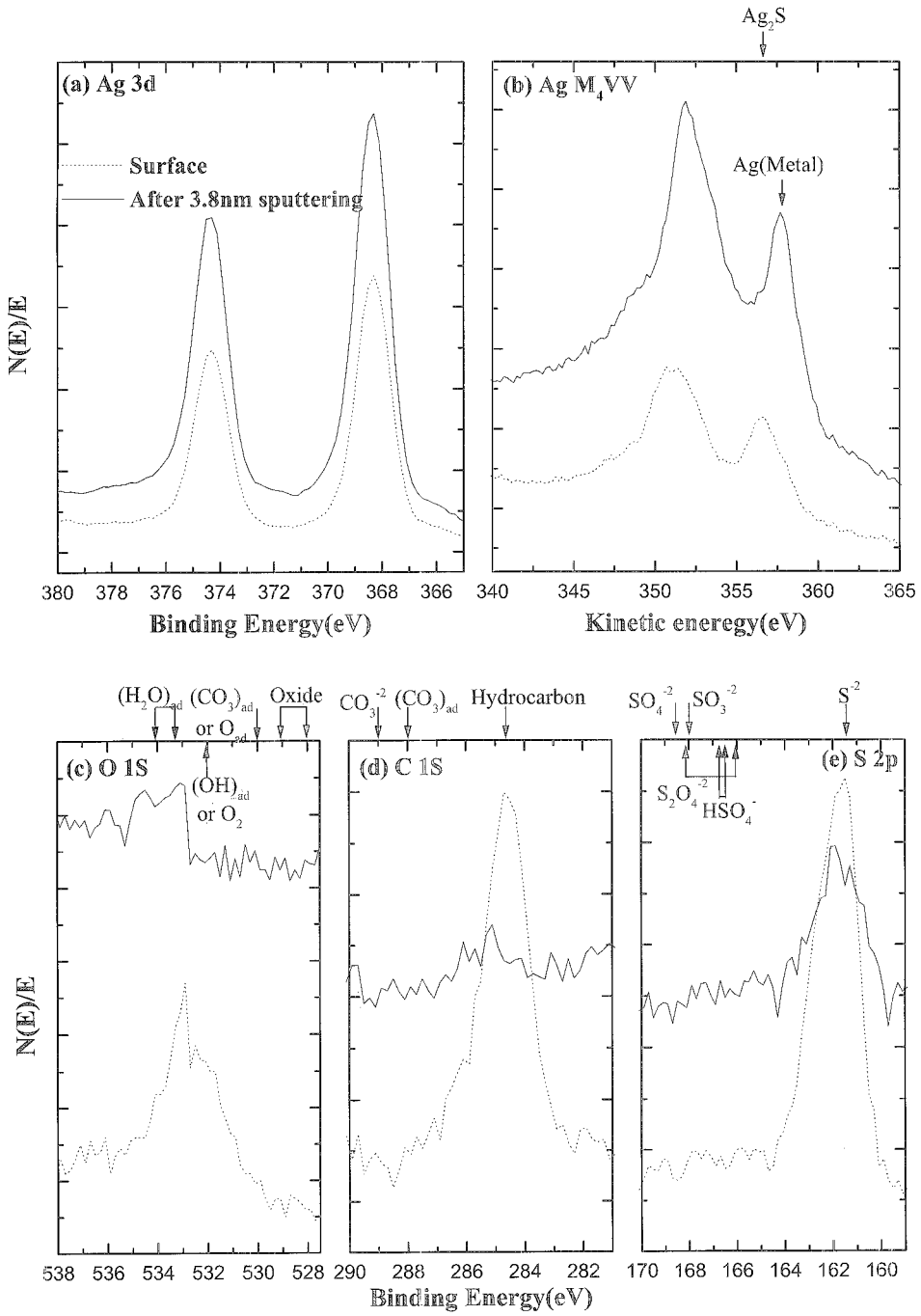

Fig. 1. XPS spectra from silver exposed to 100 ppb H_2S and 75% R.H. air for 72 hours (dot line: surface, solid line: after sputtering as deep as 3.8nm): (a) Ag-3d, (b) Ag-M_4VV, (c) O-1s, (d) C-1s, (e) S-2p

sputtering. The XPS spectra of the tarnish film formed on silver exposed to 100 ppb H_2S with air containing 15% R.H. for 90 hours were similar to in Fig. 1 except for the sulfur-2p shown in Fig. 2 indicating the presence of sulfite. The silver peaks and sulfur peaks identify the tarnish film as silver sulfide and the adsorbed species on the surface as mentioned before. Sulfite was not detected on tarnish film of silver exposed to 100 ppb H_2S with air containing 15% R.H. for less than 90 (40 hours). Hence, the sulfite is thought to be produced during exposure as long as 90 hours. The XPS spectra of the tarnish film formed on the silver exposed to 100ppb H2S with nitrogen gas containing 75% R.H. for 72 hours were similar to in Fig. 1 except for the silver peak shown in Fig. 3. The Auger parameter of silver did not match that of silver or silver sulfide and was positioned in the middle

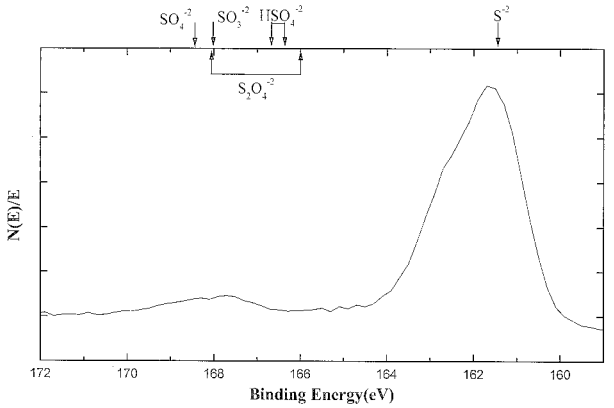

Fig. 2. Sulfur-2p spectrum from the surface of silver exposed to 100 ppb H_2S and 15% R.H. air for 90 hours

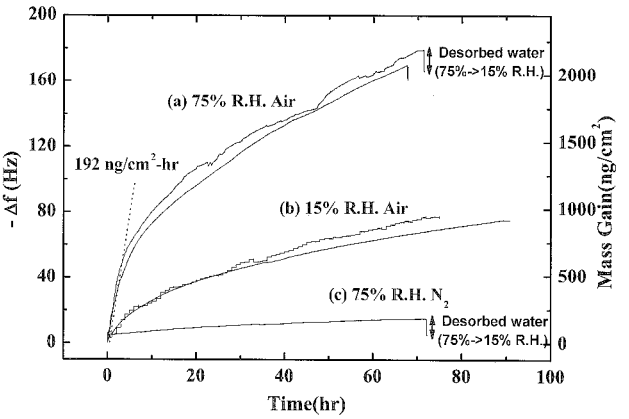

Fig. 4. Mass gain vs. time when silver coated crystals were exposed to environments containing 100 ppb H_2S: (a) 75% R.H. air, (b) 15% R.H. air, (c) 75% R.H. N_2

of these Auger parameters. Hence, the mismatch between the Auger parameter obtained and that of silver sulfide is thought to be due to that the film is thinner than the escaping depth of electron having the kinetic energy of approximately 360eV ($\approx$ 2nm)[12] or that sulfide is adsorbed on silver surface rather than chemically bonded.

Hence, the tarnish film after exposure to environments containing H_2S consisted of only silver sulfide covered by adventitious carbon, adsorbed water and possibly adsorbed oxygen and $(OH)_{ad}$.

3.2 Measurement of mass gain with QCM

Fig. 4 shows the mass gain with time when silver coated crystals were exposed to environments containing hydrogen sulfide. The mass loss occurred after the exposure condition changed from 100 ppb H_2S with 75% R.H. air (or N_2) to 15% R.H. air, indicating water desorption (120ng/cm^2) which was 1.7 times greater than that of adsorbed water (70ng/cm^2) on as-received silver metal. It may be due to the different in hydrophile property between silver and silver sulfide. In addition, Fig. 4 shows that adsorbed water enhances the tarnish rate of silver and that the presence of oxygen is required for the sulfidation of silver. Especially, no corrosion of silver in N_2 environments means that sulfide peak in Fig. 3 results from

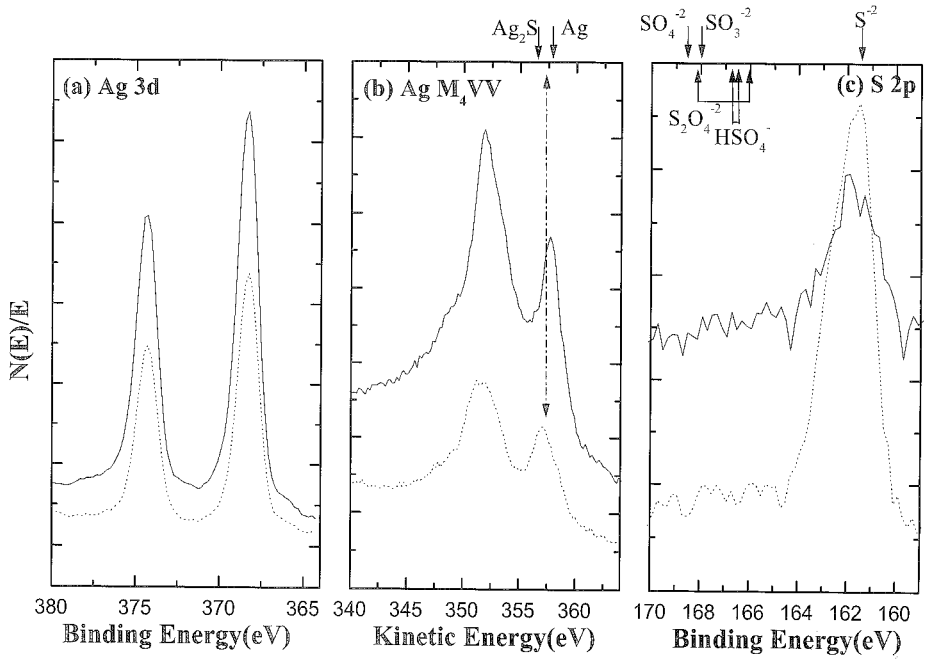

Fig. 3. XPS spectra from silver exposed 100 ppb H_2S and 75% R.H. N_2 for 72 hours (dot line: the surface, solid line: after sputtering as deep as 0.6nm): (a) Ag-$3d_{5/2}$, (b) Ag-M_4VV, (c) S-2p

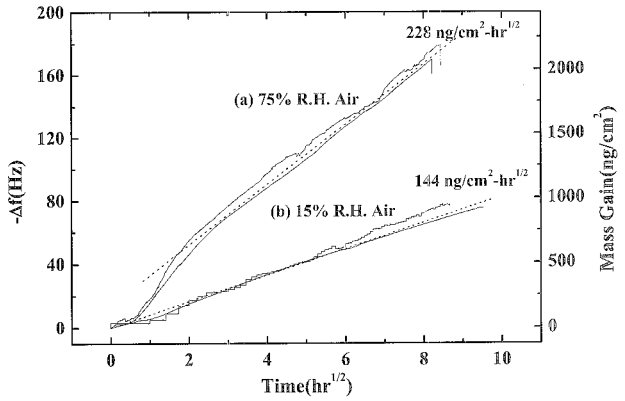

Fig. 5. Mass gain vs. time$^{1/2}$ when silver coated crystals were exposed to environments containing 100 ppb H_2S: (a) 75% R.H. air, (b) 15% R.H. air

adsorbed sulfide instead of silver sulfide. The curve (a) and the curve (b) in Fig. 4 were plotted versus time$^{1)-2)}$ scale instead of time scale in Fig. 5. The mass gain in 100 ppb H_2S with 75% R.H. air increased linearly until 8 hours after the exposure, but its rate was reduced after this period, conforming to parabolic behavior. However, in 100 ppb H_2S with 15% R.H. air, the mass gain increased only parabolically without an initial linear region. In 100 ppb H_2S with air containing 75% R.H., the kinetic behavior is due to the change of the rate determining step from surface reaction, mass transport in the gas phase or the mixed step to mass transport through the tarnish film. The reaction mechanism or transport mechanism through the tarnish film will be discussed in the next section.

3.3 Observation of morphology with FESEM

The surface morphologies of the tarnish films after exposure to various environments containing 100 ppb H_2S were the same as the surface morphology of the silver coated crystal at 100 K magnifications. Hence, the tarnish film is thought to form on the silver surface uniformly.

3.4 Phase Prediction

Fig. 6 shows the E-pH diagrams in Ag-H_2O-100 ppb H_2S system obtained from the method suggested by Zappia.[13),14)] In solid phase, silver metal, silver sulfide and silver sulfate were predicted as stable phases depending on potential, while in liquid phase silver ion, sulfite, sulfate are predicted as the stable species depending on potential. To calculate the concentrations of dissolved species (Ag^+, HS^-, S^{2-}) and equilibrium potentials ($E_{Ag^+/Ag}$, E_{H^+/H_2}), the following charge balance equation is set up under assumption that the concentration of carbon dioxide and hydrogen is 1.8 ppm and 500 ppb, respectively.

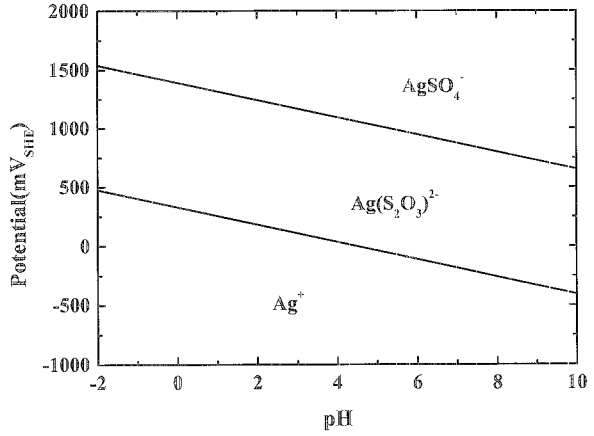

(a) Liquid phases

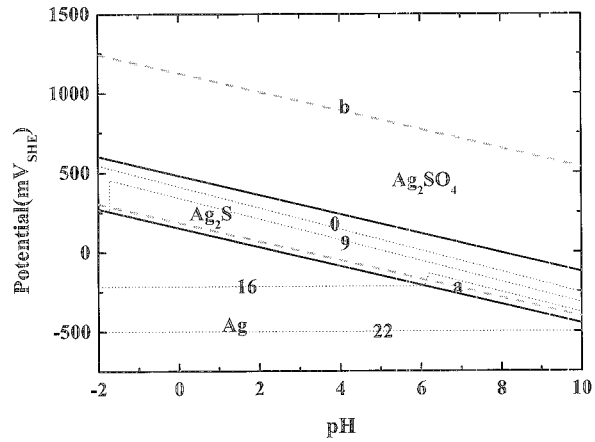

(b) Solid phases

Fig. 6. The prediction of stable phases in Ag-100 ppb H_2S-H_2O: (a) Liquid phases, (b) Solid phases, (dot line: total activity of dissolved silver (-log[Ag^+]$_T$), line a: E_{H^+/H_2}, line b: $E_{O_2/O^{2-}}$)

$$[Ag^+]+[H^+]=[HCO_3^-]+2\times[CO_3^{-2}]+[HS^-]+2\times[S^{-2}]+[OH^-] \quad (4)$$

In addition silver is thought to be corroded as only a form of silver sulfide observed according to the XPS results. Hence, the concentration of dissolved silver ion was expressed using solubility product of silver sulfide and dissolved species in equation (4) were be expressed as the concentration of hydrogen ion and the equilibrium constants listed in Table 1, finally to yield equation (5).

$$\sqrt{\frac{[H^+]\cdot Ks.p.}{P_{H_2S}\cdot K_{HH_2S}\cdot K_{d1H_2S}\cdot K_{d2H_2S}}}+[H^+]=P_{H2S}\cdot K_{HH2S}\left(\frac{K_{d1H_2S}}{[H^+]}+2\frac{K_{d1H_2S}\cdot K_{d2H_2S}}{[H^+]^2}\right)$$
$$+P_{CO_2}\cdot K_{HCO_2}\left(\frac{K_{d1CO_2}}{[H^+]}+2\frac{K_{d1CO_2}\cdot K_{d2CO_2}}{[H^+]^2}\right)+\frac{K_w}{[H^+]} \quad (2)$$

, where P_{H_2S} and P_{CO_2} is 100 ppb and 1.8ppm, respectively.

Equation (5) gave the concentrations of dissolves species

Table 1 Equilibrium constants[8]

Equilibrium constants		Value	Chemical equations
Henry's constants	K_H for CO_2	3.4×10^{-2}	$[CO_2]/P_{CO2}$
	K_H for H_2S	$10^{-0.99}$	$[H_2S]/P_{H2S}$
Dissociation constants	K_{d1} for CO_2	$10^{-6.35}$	$[H^+]\cdot[HCO_3^-]/[CO_2]$
	K_{d2} for CO_2	$10^{-10.33}$	$[H^+]\cdot[CO_3^{-2}]/[HCO_3^-]$
	K_{d1} for H_2S	10^{-7}	$[H^+]\cdot[HS^-]/[H_2S]$
	K_{d2} for H_2S	10^{-14}	$[H^+]\cdot[S^{-2}]/[HS^-]$
	K_w for H_2O	10^{-14}	$[H^+]\cdot[OH^-]$
Solubility product	$K_{s.p.}$ for A_2S	10^{-50}	$[Ag^+]^2\cdot[S^{-2}]$

(Ag^+, HS^-, S^{2-}) and the equilibrium potentials ($E_{Ag^+/Ag}$, E_{H^+/H_2}) in Fig. 7. The pH was almost independent of the concentration of hydrogen sulfide. $E_{Ag^+/Ag}$ decreased with of hydrogen sulfide, while E_{H^+/H_2} increased with of hydrogen sulfide. Especially, at 100 ppb H_2S, the difference between $E_{Ag^+/Ag}$ and E_{H^+/H_2} was as small as 8 mV though E_{H^+/H_2} was higher than $E_{Ag^+/Ag}$. Hence, choosing more correct values of activities and the concentrations of hydrogen and carbon dioxide in air may cause $E_{Ag^+/Ag}$ to be higher than E_{H^+/H_2}. In this case, it accounts for the reason why silver is not corroded by hydrogen gas though reaction in equation (6) is favorable with a viewpoint of thermodynamics.

$$Ag + H_2S\ (100ppb) \rightarrow Ag_2S + H_2\ (500ppb)\quad \Delta G = -3034J \qquad (6)$$

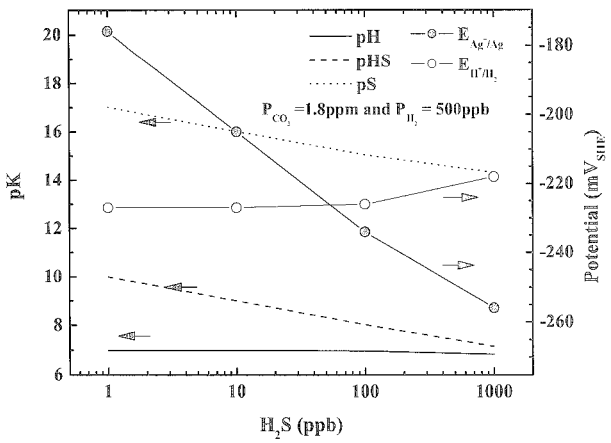

Fig. 7. The concentrations of dissolved species, such as $[H^+]$, $[HS^-]$, $[S^{2-}]$, and the equilibrium potentials of Ag^+/Ag and H^+/H_2 in aqueous electrolyte under H_2S of the range between 100 ppb and 1000 ppb

4. Discussion

The analysis of tarnish films in three different environments indicates that the overall film consisted of only silver sulfide covered by adventitious carbon, adsorbed water and possibly adsorbed oxygen and $(OH)_{ad}$. The solid film phase detected by XPS did not same as silver sulfate, the thermodynamically predicted phase in Ag-H_2S-O_2 or Ag-H_2S-O_2-H_2O ($\Delta G_{Ag_2SO_4} < \Delta G_{Ag_2S}$). T. Kuhn and G.H. Kelsall[3] reported that the discrepancy was explained by the large activation barrier for transition from silver sulfide to silver sulfate. However, it could not explain the following results: (a) the presence of sulfite on the surface after exposure in low humid environments in Fig. 2, (b) the presence of sulfide only after exposure in high humid environments in Fig. 1-(c). The adsorbed water is reported to play an important role to transport species on surface.[15),16)] In other words, the adsorbed water makes it easy to move species so that more silver ion can be fed across the film in Fig. 8 if the tarnish rate is controlled by the transport of silver across the film. The assumption mentioned just before can be justified the following facts: (a) the film growing parabolically in Fig. 5, (b) silver sulfide being a good electronic conductor as well as an good ionic conductor (*i.e.*, $\kappa_{Ag2O}\approx10^{-8}\ \Omega^{-1}\text{-cm}^{-1}$, $\kappa_{Ag2S}\approx10^{-8}\ \Omega^{-1}\text{-cm}^{-1}$),[17),18)]

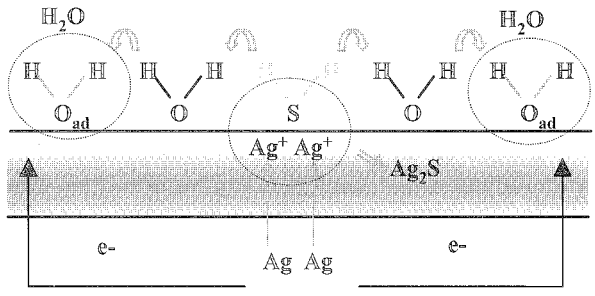

Fig. 8. The tarnish process of silver exposed to humid air (high R.H.) containing H_2S[16]

(c) silver is a dominant species for ionic conduction due to higher diffusivity,[19),20)] (d) the uniform growth according to FESEM observation. Hence, the surface coverage of water increases the effective anodic area so that the oxidizing power decreases. This proposal gives a key to explain the presence of sulfite after low humid exposure but no detection of sulfite after high humid exposure. In addition, the stable solid phase (Ag_2S, Ag_2SO_4) depending on potential as shown in Fig. 6 is agreed with the proposal and XPS results.

Considering measurements of tarnish rate in environments without oxygen in Fig. 4-(c), silver and hydrogen sulfide in high humid environments, reacts each other as follows and the film uniformly grows in Fig. 8:

Anodic reaction (at m/f interface):

$$Ag \rightarrow Ag^{+} + e^{-} \qquad E = -225mV \qquad (7)$$

Cathodic reaction (at f/s interface):

$$1/2H_2O + 1/4O_2 + e^{-} \rightarrow OH^{-} \qquad E = 804mV \qquad (8)$$

Overall reaction:

$$2Ag + H_2S + 1/2O_2 \rightarrow Ag_2S + H_2O \qquad (9)$$

In this study, the tarnish rate was not measured unfortunately in real dry environments so that the effect of water on the tarnish rate like oxygen is not known. However, the tarnish rate is thought to be much smaller.

It was explained with Oakes's proposal[21)] that silver could not be oxidized by molecular oxygen, but by atomic oxygen. However, low tarnish rate in real dry environments is more reasonably supposed to be necessary to transport reactive species on surface in Ag-H_2S unlike Ag-H_2S-NO_2 system.[15),16)]

5. Conclusions

From the calculation of phase equilibrium, XPS analysis and weight measurements, the tarnish process of silver is an electrochemical process in an bulk aqueous solution, where oxygen is reduced to hydroxide, and oxidized silver (Ag^{+}) reacts with dissociated hydrogen sulfide to form silver sulfide, and a growth process of sulfidation film which silver ion or sulfide is transported across. The adsorbed water provided a role of media for transporting dissolved species such as hydroxide and dissociated hydrogen sulfide and a site for electrochemical reaction to enhance tarnish rate.

References

1. J. Guinement and C. Fiaud, *13th Inter. Conf. on Electric Contacts*, p. 383, Lausanne (1986).
2. D. Simon, C. Perrin, D. Mollimard, M. T. Bajard, and J. Bardolle, *13th Inter. Conf. on Electric Contacts*, p. 333, Lausanne (1986).
3. T. Kuhn and G. H. Kelsall, Corrosion of Electrical Contacts, p. 51, Institute of Metals, Great Britain (1989).
4. W. H. Abbott, *Proc. 4th Int. Res. Symp. Electrical Contact Phemonena*, p. 35, Swansea (1968).
5. T. E. Graedel, J. P. Franey, G. J. Gualtieri, G. W. Kammlott and D. L. Malm, *Corr. Sci.*, **25**, 1163 (1985).
6. L. Volpe and P. J. Peterson, *Corr. Sci.*, **29**, 1179 (1989).
7. P. B. P. Phipps and D. W. Rice, Corrosion Chemistry, p. 235, G. R. Brubaker and P.B.P. Phipps(Eds.), Washington (1979).
8. H. Kim, Ph. D. Thesis, Case Western Reserve University, Cleveland, OH (1996).
9. D. W. Rice, E. B. Rigby, P.B.P. Phipps, R. J. Cappell and R. Tremoureux, *J. Electrochem. Soc.*, **128**, 275 (1989).
10. D. A. Buttery, Electroanalytical Chemistry vol. 17, A. J. Bard, (Ed.), p. 1, Marcel Dekker Inc., New York (1989).
11. S. Bruckenstein and S. Swathirajann, *Elecrochemica Acta*, **30**, 851 (1985).
12. M. P. Seah and W. A. Debch, *Surf. and Interface Anal.*, **1**, 2 (1979).
13. J. C. Angus, B. Lu, and M. J. Zappia, *J. Appl. Electrochem.*, **17**, 1 (1987).
14. J. C. Angus and M. J. Zappia, *J. Electrochem. Soc.*, **134**, 1374 (1987).
15. J-E Svensson and L-G Johansson, *J. Electrochem. Sci.*, **143**, 51 (1996).
16. H. Kim, *Materials and Corrosion*, **54**, 243 (2003).
17. T. Nomura, T. Nagamunne, K. Izutsu, and T. S. West, Bunseki KagaKu, **30**, 494 (1981).
18. Yu. G. Vlasov and Yu. E. Ermolenko, *Elektrokhemiya*, **17**, 1301 (1981).
19. D. Grientsching and W. Sitte, *J. Phys. Chem. Solids.* **52**, 805 (1991).
20. R. L. Allen and W. J. Moore, *J. Chem. Phys.*, **63**, 223 (1985).
21. D. B. Oakes, *J. Appl. Phys.*, **77**, 2166 (1995).